THE BELL SYSTEM TECHNICAL JOURNAL
Vol. 56, No. 3, March 1977
*Printed in U.S.A.*

# 100-GHz Measurements on a Multiple-Beam Offset Antenna

By R. A SEMPLAK

(Manuscript received September 8, 1976)

*Large-capacity satellite communication systems can be developed by equipping both satellites and earth stations with multiple-beam antennas. Such antennas can be produced from an offset Cassegrain with offset collectors as feeds.*

## I. INTRODUCTION

Large-capacity satellite communication systems can be achieved by equipping both the satellites and earth stations with multiple-beam antennas.[1] An offset Cassegrainian antenna (Fig. 1) fed by multiple, but separate, small corrugated horns has been proposed for such a system.[2] Measurements and theory have indicated that the offset geometry results

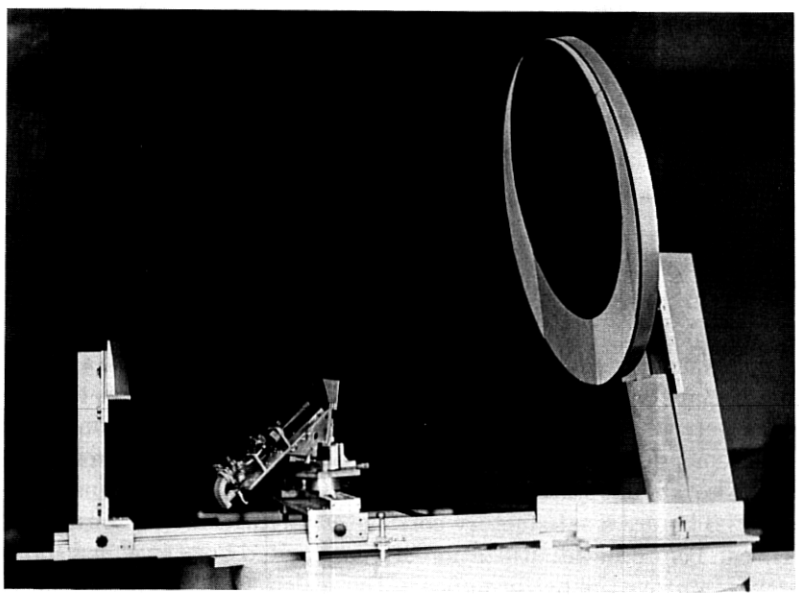

Fig. 1—100-GHz beam-scanning antenna.

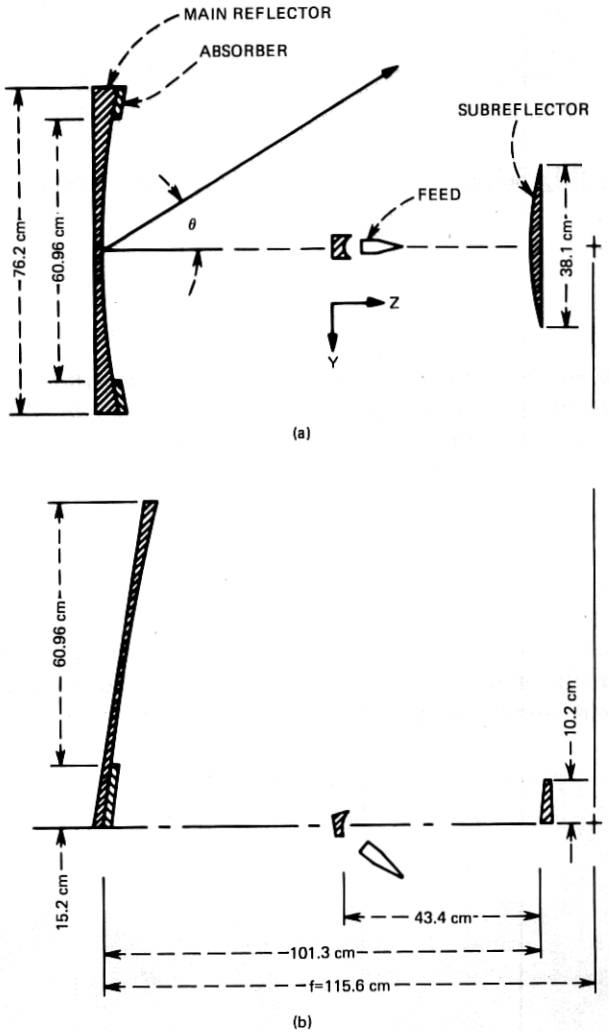


Fig. 2—Plan view of 100-GHz beam-scanning antenna. (a) Plan view. (b) Side view.

in an ideal configuration[3–5] for both earth-station and satellite antennas since the aperture has no blockage; this significantly reduces the side-lobe levels and, in turn, reduces adjacent station interference. The measurements to be discussed here were obtained with a dual-mode feed horn. The current state-of-the-art needs to be pushed to its maximum potential before a satisfactory corrugated (hybrid-mode) horn at 100 GHz can be produced; utilization of a corrugated horn as a feed should further improve the performance of the scaled model discussed here.

This 100-GHz exploratory study utilizes an antenna that scales to about 2 m at about 30 GHz on a satellite (shown in Fig. 1). The antenna consists of a 60.96-cm-diameter, numerically machined, parabolic section on the right; a confocal 38.1-cm-wide by 10.2-cm-high, numerically machined, hyperbolic subreflector on the left; and in the center, an offset collector feed that consists of a 5.08-cm, numerically machined, parabolic reflector illuminated by a dual-mode horn. The feed is mounted on a

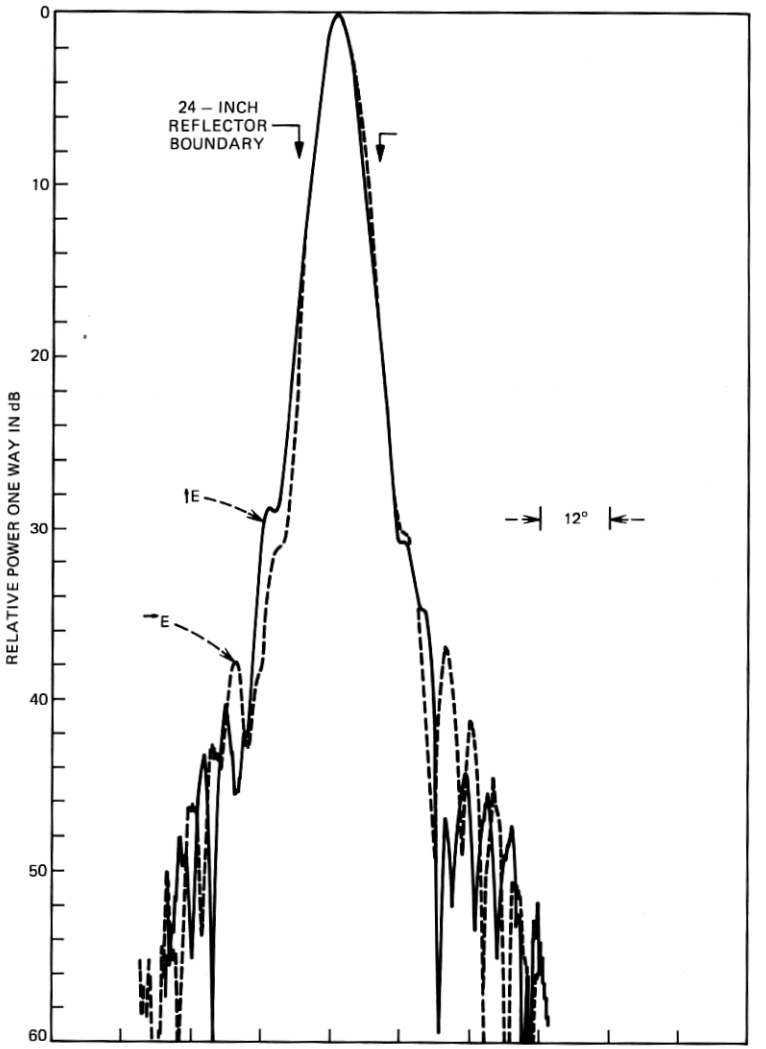


Fig. 3—Far-field radiation patterns of the offset collector feed for the principle linear polarization.

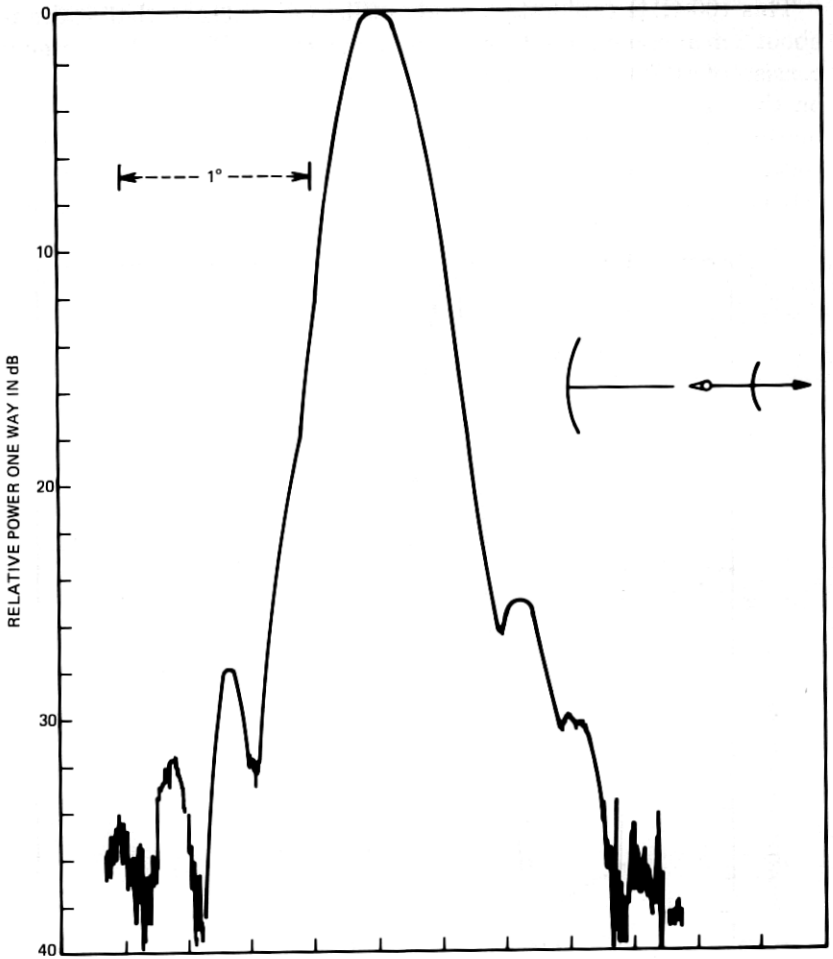


Fig. 4—Azimuth scan of the far-field radiation pattern of the antenna for zero feed displacement (y = 0, z = 0); this is the reference position $\theta = 0°$.

device that provides coarse and fine adjustments in both the $y$ and $z$ axis (into the plane of the photograph and along the axis of the main paraboloid, respectively). Fine adjustments are provided in the direction of the $x$ axis and rotation about this axis is also provided.

The 60.96-cm-diameter main reflector was obtained by reducing a 76.2-cm-diameter reflector with absorbing material whose one-way transmission loss at 100 GHz is of the order 26 dB. The absorber is positioned as shown in Fig. 1 to avoid blockage. Hence, contributions to the far-field radiation pattern from the masked area are small.

Figures 2a and 2b are the plan view and side view, respectively, of the scale model showing various dimensions. From these dimensions, we observe that the aperture is large in wavelengths and the $f/D$ (i.e., the ratio of prime focal length to diameter) is large, 1.9; hence, we should be able to scan tens of beamwidths by lateral displacement of the feed.[6]

The radiation characteristics of the feed, shown in Fig. 3, are for the principle linear polarizations in the azimuthal plane. We observe from this figure that the amplitude is very similar for both polarizations. The tick marks on this figure, which denote the edges of the apodized main reflector, indicate an illumination taper of the order 18 dB.

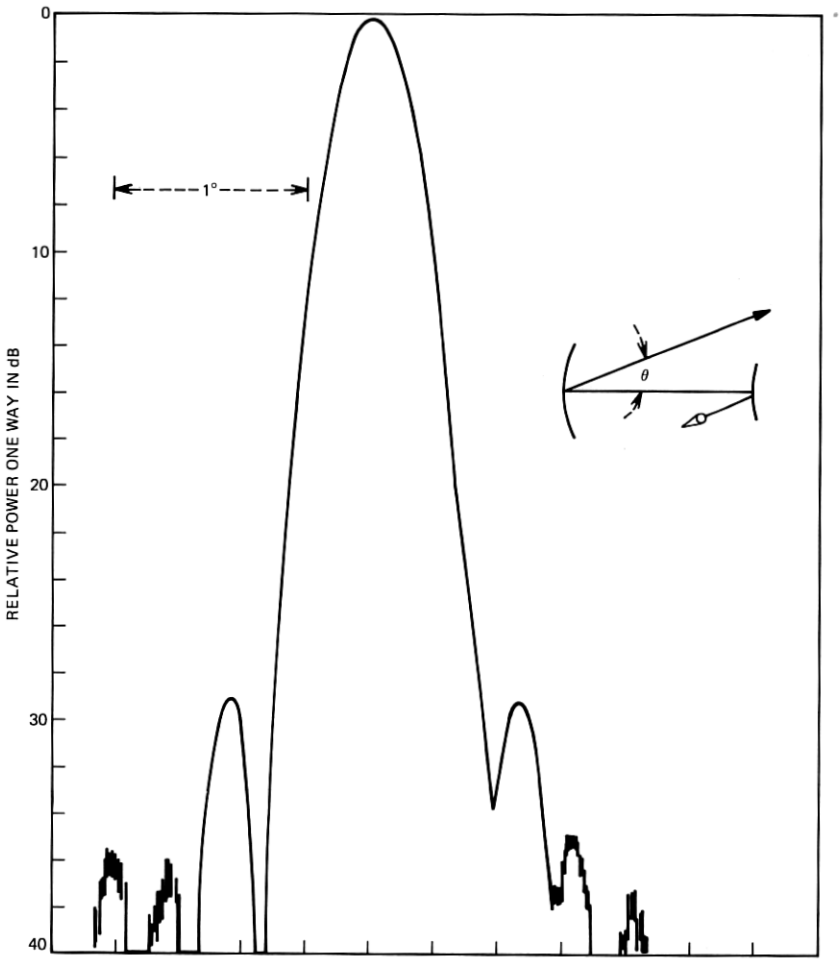


Fig. 5—Azimuth scan with beam displaced $\theta = 3.4°$.

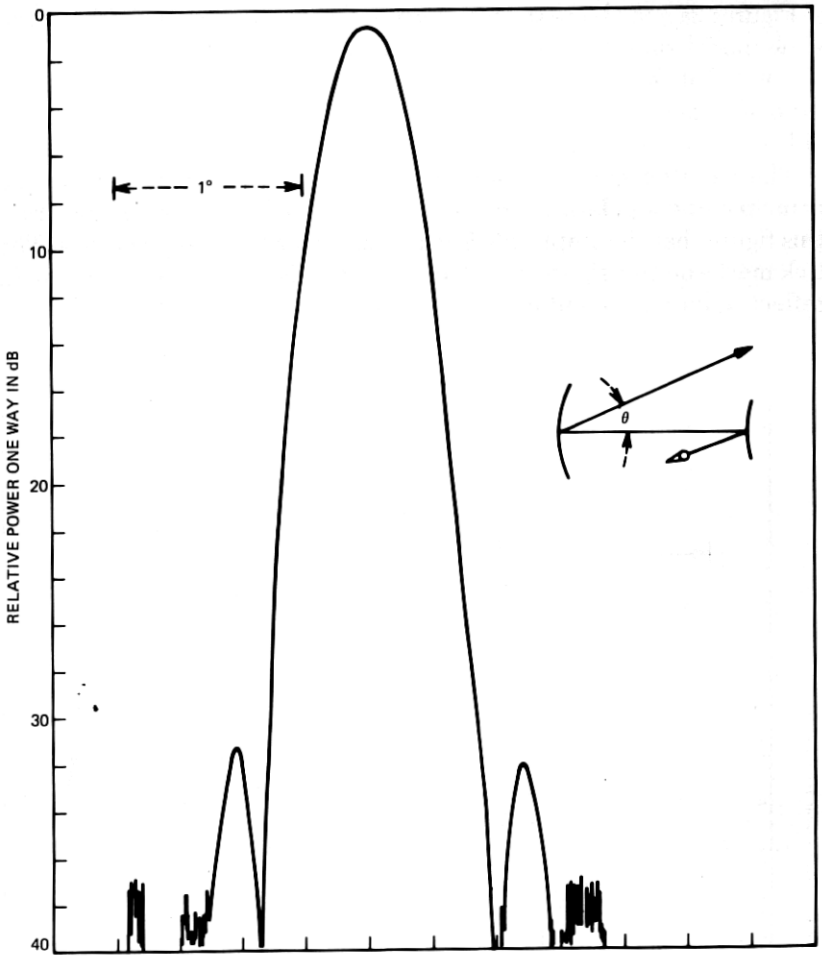


Fig. 6—Azimuth scan with beam displaced $\theta = 4.3°$.

## II. FAR-FIELD RADIATION MEASUREMENTS

As determined by using Bell Laboratories radio range, measurement of the incident field presented to the aperture of the beam-scanning antenna indicates an amplitude variation of the order 0.5 dB. Also, variations in the refractive index of the air along the 480-meter range produce scintillations. These scintillations are time-of-day dependent and their effects were minimized by measuring in the early morning and late afternoon. Overcast days were ideal. The siting of the antenna is such that radiation-pattern measurements in the elevation plane are perturbed by ground reflections and therefore are not discussed.

The measurements shown in Figs. 4 through 11 are made in the azimuthal plane for vertical polarization. For Fig. 4, the feed is on axis and all subsequent beam-scanning measurements are referred to the on-axis measurement. Here in Fig. 4, we see a well-behaved far-field pattern with side lobes about 27 dB down located two and one-half beamwidths from axis. The insert of this figure is a sketch showing the relative location of the feed with respect to the subreflector and main reflector. The arrow indicates the direction of the transmitting source.

Figures 5 through 10 show measurements obtained by displacing the feed laterally ($y > 0$). The feed was adjusted in all its degrees of move-

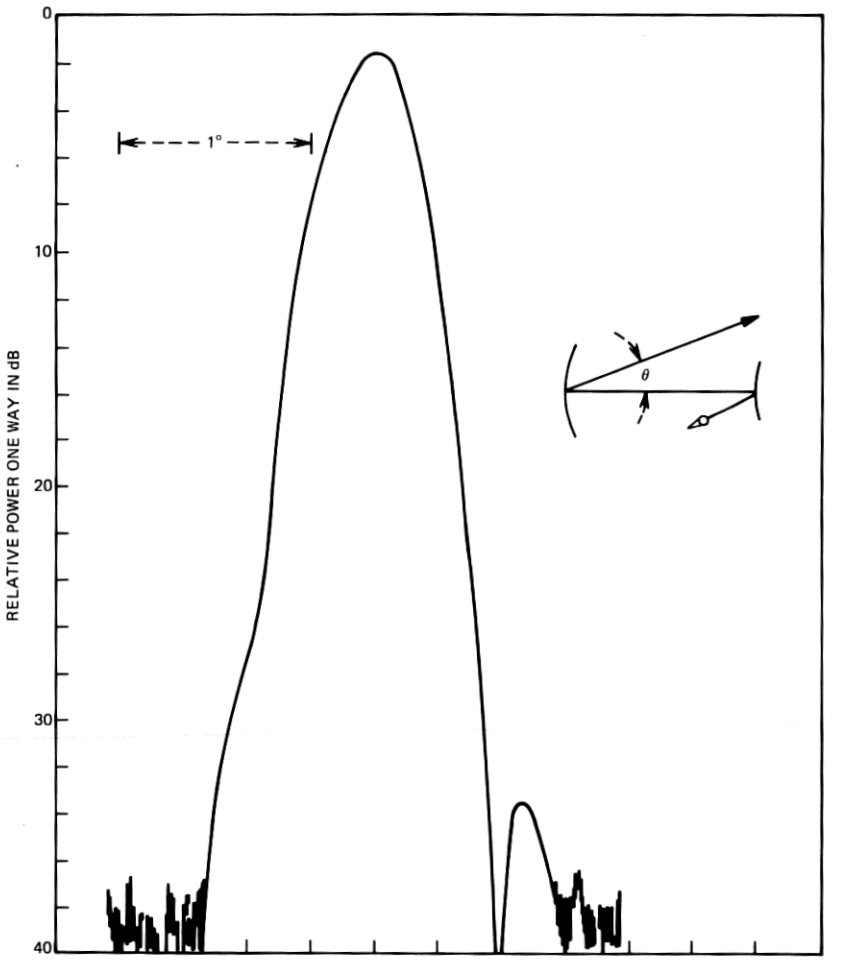


Fig. 7—Azimuth scan with beam displaced $\theta = 5.0°$.

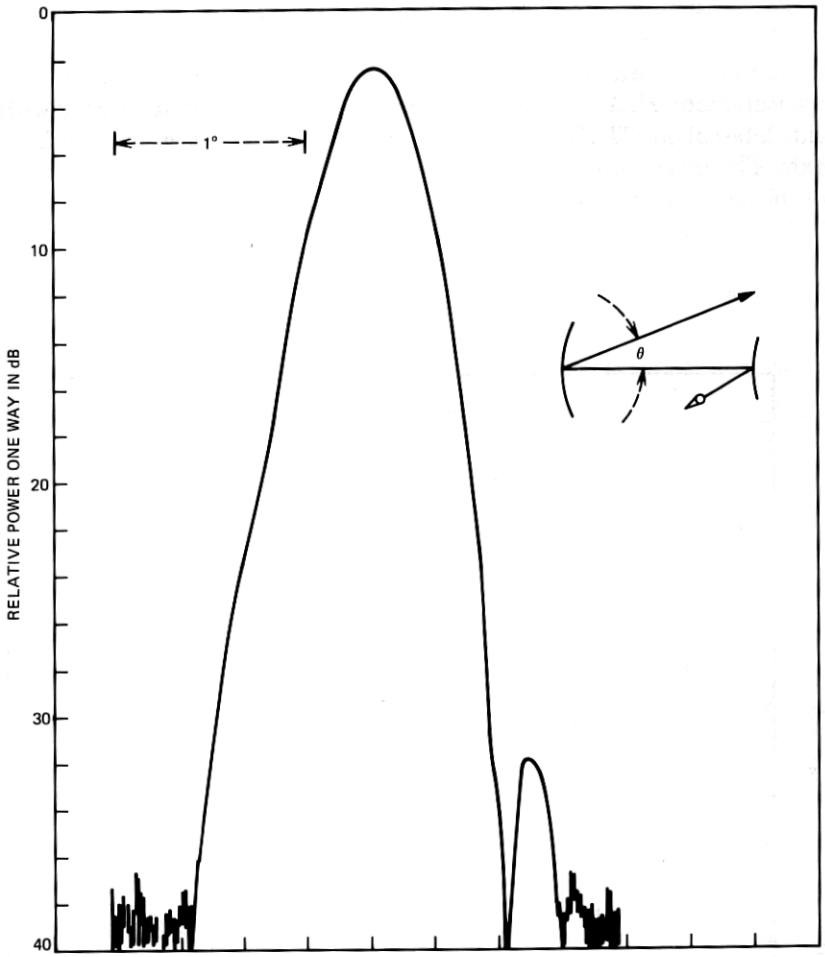


Fig. 8—Azimuth scan with beam displaced $\theta = 6.25°$.

ment to optimize the gain for each displacement of the feed, including $x$ and $z$. The angular beam displacement $\theta$ is indicated on each figure. We observe the decrease in gain (at zero angle) and also that the side lobes continuously decrease with increase in scan angle.

Measurements were also made by displacing the feed in the opposite direction ($y < 0$) and Fig. 11 is typical; this pattern is almost mirror symmetric to that of Fig. 7. One notes the similarity and therefore concludes that the feed is on the electrical axis of the antenna for the $\theta = 0$ pattern. Further examination and comparison of Figs. 4 through 11 disclose the lack of deep minima for the first nulls of the on-axis position

(Fig. 4); the minima are much more pronounced in Figs. 5 and 6. Improvement in performance for the "on-axis" position was explored by moving the feed in small increments, but the absence of sharp nulls for this reference position (Fig. 4) can not be explained at this time.

### III. BEAM-SCANNING MEASUREMENTS

Figure 12 is a plot of gain (relative to the on-axis gain) versus scan angle. The footed vertical bars indicate the maximum and minimum gain measured for the indicated scan angle. The solid dot is the average of

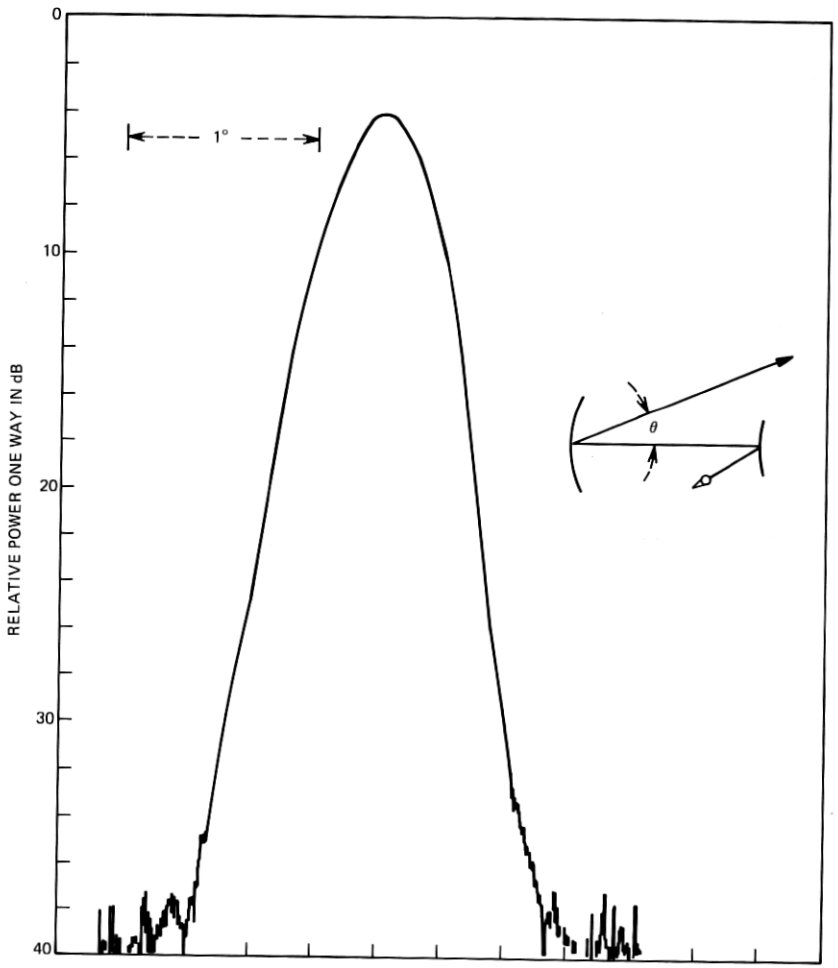


Fig. 9—Azimuth scan with beam displaced $\theta - 7.24°$.

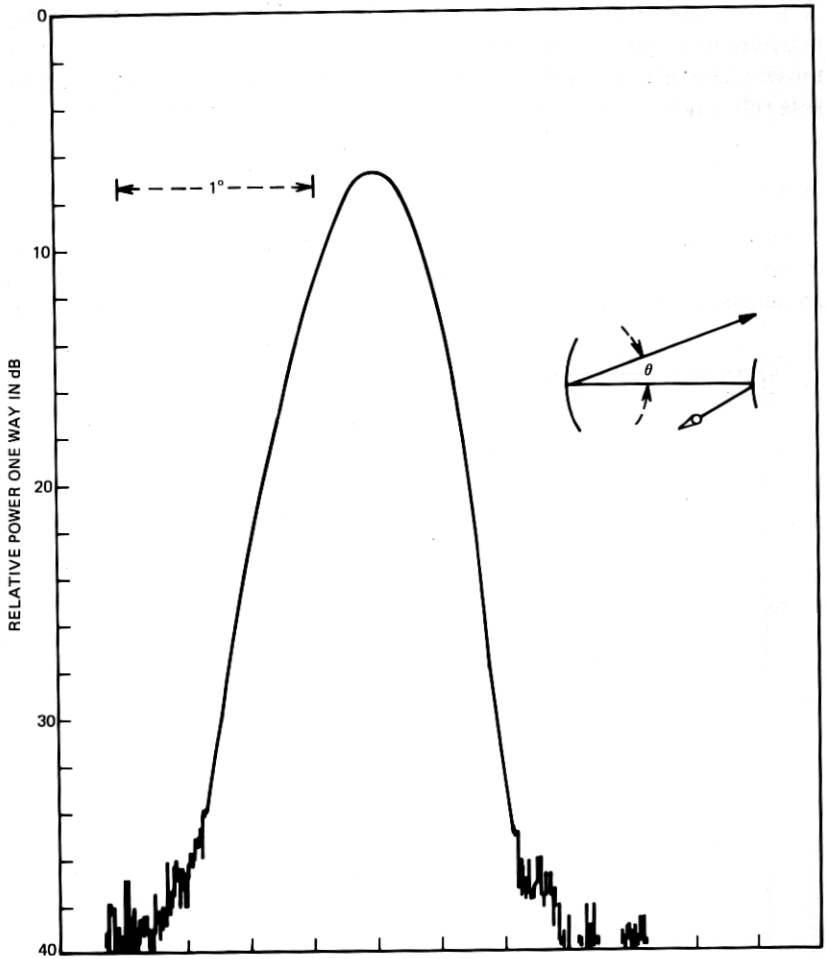


Fig. 10—Azimuth scan with beam displaced $\theta - 8.01°$.

measurements within a 0.2 degree interval. The open circles, measurements made in the opposite scan direction ($y < 0$), are similar to those for $y > 0$. Scan-angle measurements of less than 3 degrees were not made since the change in relative gain is small. The curve is well behaved out to a scan angle of 4.5 degrees (of the order of 12 beamwidths). Many measurements were made in the region of 4.5 to 6.0 degrees to confirm the presence of the shoulder in the curve. Clearly, the antenna can be scanned ±3.5 degrees (18 beamwidths) with degradation in gain of only 0.25 dB. A scan of ±4.5 degrees (24 beamwidths) degrades the gain only 1 dB. Thus, the contiguous United States could be served by a syn-

chronous satellite with a multiple-beam antenna of this type and suffer less than 0.5-dB degradation of gain.

Figure 13 is a plot of feed displacement in the $y$ and $z$ directions required to optimize the gain for a given scan angle of the beam. In a sense, this is the plot of the locus of focus—it is not a straight line. It was found that no displacement in $x$ was necessary.

Figure 14 shows plots of the 3, 10, and 20-dB beamwidths as a function of scan angle; the beamwidths increase with increasing scan angle. This increase in beamwidth limits the number of feeds that can be used on this type of antenna.

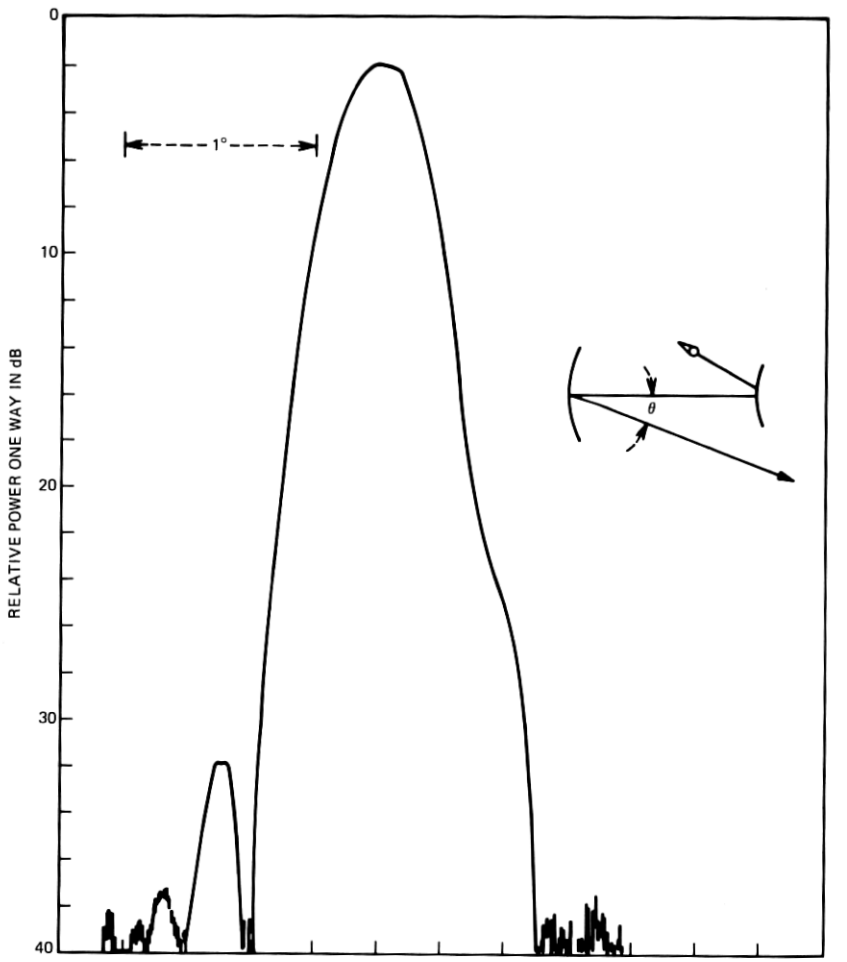


Fig. 11—Azimuth scan with beam displaced in opposite direction $\theta = -5.32°$.

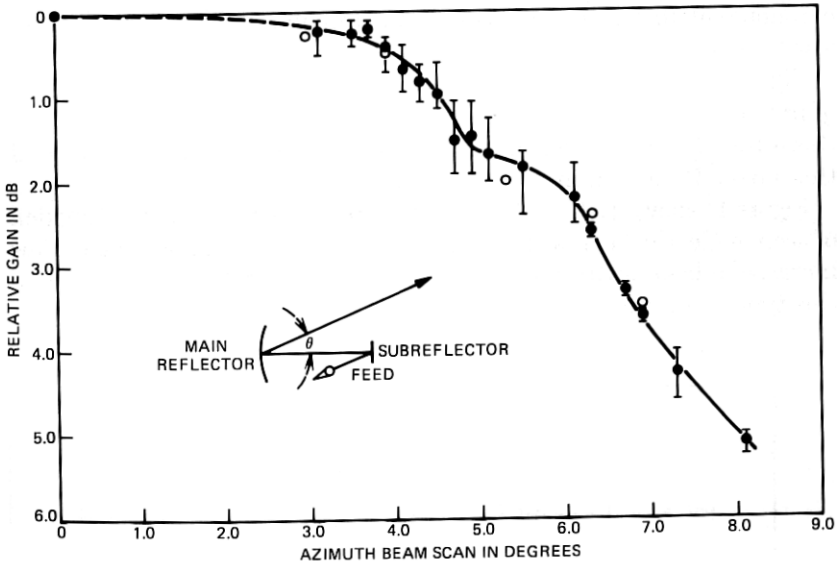


Fig. 12—Relative gain measured as a function of beam scanning $\theta$.

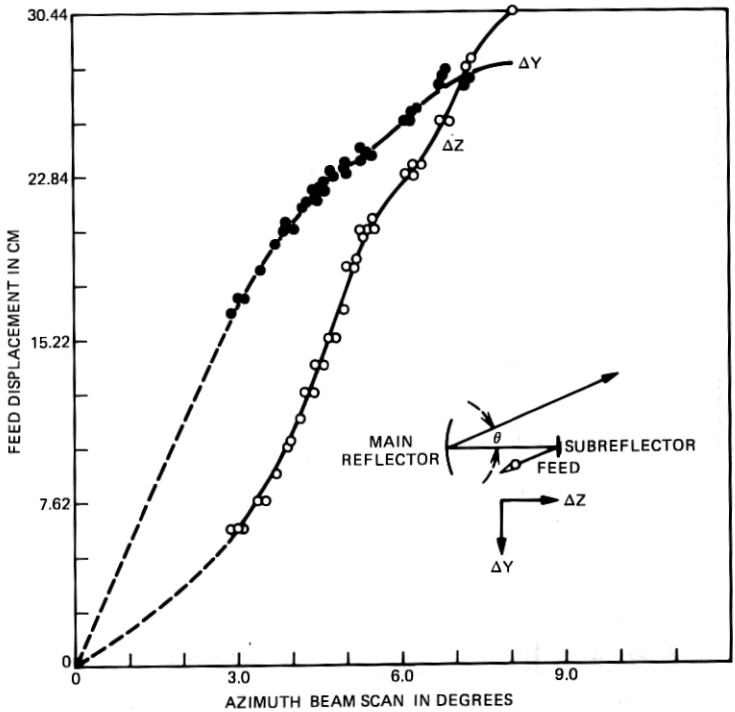


Fig. 13—Feed displacement as a function of beam scanning $\theta$.

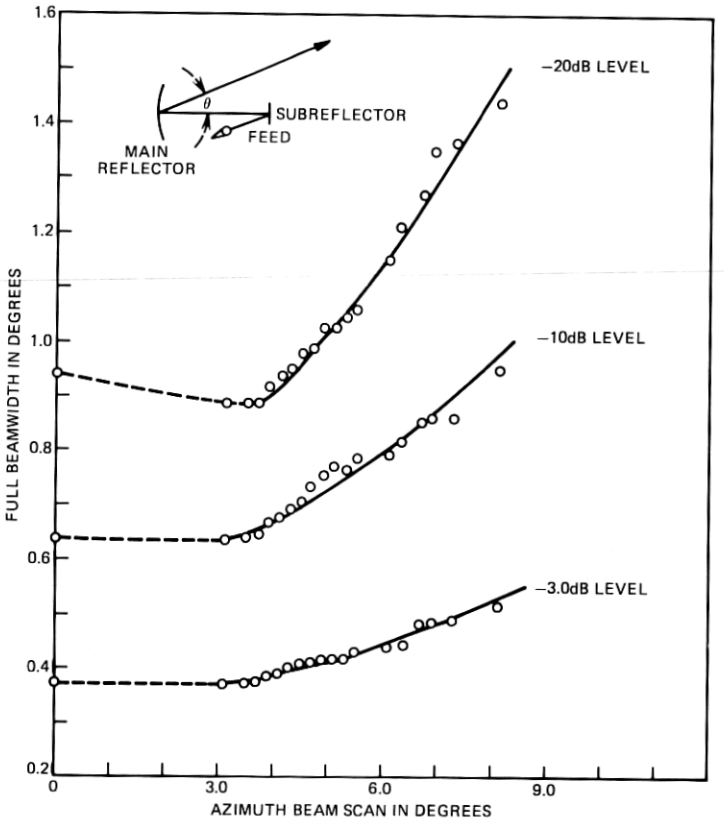


Fig. 14—Plot of 3, 10, 20 dB level beamwidths as a function of beam scanning $\theta$.

## IV. CONCLUSIONS

From the measurements, we conclude that multiple-beam antennas can be produced by using an offset Cassegrain with offset collectors as feeds. Further, they are suitable for both earth stations and satellites. We can scan a total of 18 beamwidths with only 0.25-dB degradation in gain; a scan of this order produces little change in radiation characteristics.

## V. ACKNOWLEDGMENTS

The assistance of W. E. Legg in measuring the feed system is greatly appreciated. Thanks to R. H. Turrin and E. A. Ohm for providing the subreflector, to D. A. Gray for the help with the 100-GHz equipment, and to D. C. Hogg for his encouragement.

## REFERENCES


1. L. C. Tillotson, "A Model of a Domestic Satellite Communication System," B.S.T.J., *47,* No. 10 (December 1968), pp. 2111–2137.
2. E. A. Ohm, "A Proposed Multiple-Beam Microwave Antenna for Earth Stations and Satellites," B.S.T.J., *53,* No. 8 (October 1974), pp. 1657–1665.
3. C. Dragone and D. C. Hogg, "The Radiation Pattern and Impedance of Offset and Symmetrical Near-Field Cassegrainian and Gregorian Antennas," IEEE Trans. Ant. Propag., *AP-22,* No. 3 (May 1974), pp. 472–475.
4. M. J. Gans and R. A. Semplak, "Some Far-Field Studies of an Offset Launcher," B.S.T.J., *54,* No. 7 (September 1975), pp. 1319–1340.
5. Ta-Shing Chu and R. H. Turrin, "Depolarization Properties of Offset Reflector Antennas," IEEE Trans. Ant. Propag. *AP-21,* No. 3 (May 1973), pp. 339–345.
6. John Ruze, "Lateral Feed Displacement in a Paraboloid," IEEE Trans. Ant. Propag. *13,* No. 5 (September 1965), pp. 660–665.